Brazilian Journal of Biology®

ISSN 1519-6984 (Print)
ISSN 1678-4375 (Online)

Original Article

Assessment of the potential toxic of naringenin nanoparticles using *ex vivo* and *in silico* models

Avaliação do potencial tóxico de nanopartículas de naringenina usando modelos *ex vivo* e *in silico*

G. B. Costa[a], B. F. Rossi[b], B. P. M. Oliveira[b], D. E. Santo[c], F. V. Leimann[a,d], A. L. Romero[e], A. P. Peron[c] and O. H. Gonçalves[a,d,f*]

[a]Universidade Tecnológica Federal do Paraná – UTFPR, Programa de Pós-graduação em Tecnologia de Alimentos – PPGTA, Campo Mourão, PR, Brasil
[b]Universidade Tecnológica Federal do Paraná – UTFPR, Curso de Engenharia de Alimentos, Campo Mourão, PR, Brasil
[c]Universidade Tecnológica Federal do Paraná – UTFPR, Programa de Pós-graduação em Engenharia Ambiental, Francisco Beltrão, PR, Brasil
[d]Instituto Politécnico de Bragança, Centro de Investigação de Montanha – CIMO, Campus de Santa Apolónia, Bragança, Portugal
[e]Universidade Tecnológica Federal do Paraná – UTFPR, Programa de Pós-graduação em Rede Nacional em Gestão e Regulação de Recursos Hídricos – ProfÁgua, Campo Mourão, PR, Brasil
[f]Universidade Federal de Santa Catarina, Programa de Pós-graduação em Engenharia Têxtil, Blumenau, SC, Brasil

Abstract

Naringenin is a flavonoid known for its anti-inflammatory, antineoplastic, antiatherogenic, and antioxidant properties. However, it has poor technological characteristics and limited bioavailability, which hinder its use in food applications. Nanoencapsulation could address these limitations, but safety concerns regarding nanoengineered bioactives need to be resolved before they can be effectively utilized as food additives. The objective of this study was to evaluate the potential cytotoxic, genotoxic, and mutagenic effects of both free and encapsulated naringenin through in vivo experiments using *Allium cepa* L. roots, along with pharmacokinetic and molecular docking analyses. The results showed that naringenin nanoparticles did not produce significant changes in the cell division index of meristematic cells in *A. cepa* roots. Additionally, no significant alterations in the mitotic spindle or chromosomal breaks were observed. Molecular docking studies indicated that naringenin effectively binds to the active site of the catalase enzyme (CAT) in a competitive manner, while it attaches to a site away from the active site of superoxide dismutase (SOD2), demonstrating a non-competitive interaction. ADMET property assessments suggested that naringenin exhibits relatively low toxicity and has favorable molecular characteristics for oral administration. In summary, this study supports the potential of naringenin, particularly in its nanoencapsulated form, as a safe and effective ingredient for functional foods, provided that safety concerns regarding nanoencapsulation are adequately addressed.

Keywords: cytotoxicity, genotoxicity, *Allium cepa* L., ADMET.

Resumo

A naringenina é um flavonoide conhecido por suas propriedades anti-inflamatórias, antineoplásicas, antiaterogênicas e antioxidantes. No entanto, apresenta características tecnológicas deficientes e baixa biodisponibilidade, o que dificulta seu uso em aplicações alimentares. A nanoencapsulação pode superar essas limitações, mas é necessário resolver preocupações sobre a segurança de bioativos nanoengenheirados antes que possam ser utilizados efetivamente como aditivos alimentares. O objetivo deste estudo foi avaliar os potenciais efeitos citotóxicos, genotóxicos e mutagênicos da naringenina, tanto em sua forma livre quanto encapsulada, através de experimentos in vivo com raízes de *Allium cepa* L., juntamente com análises farmacocinéticas e de docking molecular. Os resultados mostraram que as nanopartículas de naringenina não apresentaram alterações significativas no índice de divisão celular das células meristemáticas nas raízes de *A. cepa*. Além disso, não foram observadas alterações significativas no fuso mitótico ou quebras cromossômicas. Os estudos de docking molecular indicaram que a naringenina se liga efetivamente ao sítio ativo da enzima catalase (CAT) de maneira competitiva, enquanto se anexa a um local distante do sítio ativo da superóxido dismutase (SOD2), demonstrando uma interação não competitiva. As avaliações das propriedades ADMET sugeriram que a naringenina apresenta toxicidade relativamente baixa e características moleculares favoráveis à administração oral. Em resumo, este estudo apoia o potencial da naringenina, especialmente em sua forma nanoencapsulada, como um ingrediente seguro e eficaz para alimentos funcionais, desde que as preocupações de segurança relacionadas à nanoencapsulação sejam adequadamente abordadas.

Palavras-chave: citotoxicidade, genotoxicidade, *Allium* cepa L., ADMET.

*e-mail: odinei.hg@ufsc.br
Received: September 23, 2024 – Accepted: October 18, 2024

1. Introduction

Researchers worldwide have increasingly focused on the role of diet in maintaining health and preventing diseases (Silva et al., 2021). In this context, functional foods are defined as substances or components of food that provide health benefits. Naringenin, a polyphenol belonging to the flavonoid class, is primarily found in citrus fruits and can also be obtained through biotechnological processes. It offers several health benefits typical of polyphenols, including antioxidant activity, reduction of oxidative stress, and anti-inflammatory effects. However, it has low bioavailability when administered orally.

From a technological standpoint, its poor solubility in water limits its applications in the food industry. Nanoencapsulation of naringenin may be an effective strategy to enhance its biological activity (McClements, 2018; Sumathi et al., 2015) while creating a colloidally stable dispersion in water. Indeed, there has been a growing number of publications detailing the development and application of colloidal delivery systems (CDS) for food-grade active ingredients, such as vitamins, nutraceuticals, colorants, flavors, enzymes, and probiotics (McClements, 2018). Nanoparticles made from surfactants or polymers can enhance the stability of encapsulated compounds and improve their efficacy (Almeida et al., 2018). From a technological perspective, nanoparticulate systems are appealing because they can preserve the antioxidant activity of chemical substances, improve consumption experience, extend shelf life, and mitigate unpleasant flavors such as astringency and bitterness that can occur at high concentrations (Kerdudo et al., 2014).

Bioavailability is closely linked to the absorption process, and high oral bioavailability is often a critical factor in developing nutraceutical food products. One widely accepted approach to assess oral bioavailability is Lipinski's Rule of Five (Lipinski, 2004), which outlines five criteria related to solubility and permeability through the plasma membrane that must be met for a substance to be considered adequately bioavailable. Studies indicate that encapsulated naringenin has better bioavailability compared to its free form. For instance, Chaurasia et al. (2018) conducted a study aimed at enhancing the effectiveness of naringenin in combating colorectal cancer by developing a drug delivery system using polymeric nanoparticles, which demonstrated significantly higher bioavailability than the free form.

The antioxidant potential of naringenin is well-documented in the literature, demonstrating scavenging activity against superoxide anion radicals and hydroxyl radicals (Cavia-Saiz et al., 2010), his activity is attributed to naringenin's ability to enhance the expression of key antioxidant enzymes, including superoxide dismutase (SOD), glutathione peroxidase (GPx), and catalase (CAT) (Maatouk et al., 2016; Manchope et al., 2016; Vezza et al., 2016).

Superoxide dismutases (SOD) are metal-containing enzymes that play a crucial role in human health by acting as essential antioxidants. They scavenge reactive oxygen species, particularly the superoxide anion, and serve as a primary defense mechanism against the harmful effects of oxidative stress by facilitating the detoxification of its byproducts. Dysfunction or reduced activity of SODs has been linked to various human diseases (Johnson and Giulivi, 2005). Among the different isoforms of superoxide dismutase in mammals, SOD2 is particularly significant in the context of neurodegenerative diseases. Superoxide is generated as a byproduct of oxidative phosphorylation when molecular oxygen enters the mitochondria. SOD2 helps mitigate the harmful effects of superoxide by converting it into hydrogen peroxide, which can diffuse from the mitochondrion and be further detoxified into water by antioxidant enzymes like catalase (Flynn and Melov, 2013). Thus, catalase is another important enzyme to consider.

Catalase is central to defending against oxidative damage and inactivating hemoglobin in erythrocytes, relying on a heme-dependent catalytic cycle. In the brain, the reaction of ethanol with catalase is a significant source of acetaldehyde, which is associated with the neurological effects of alcohol in humans. Treatment with the catalase inhibitor 3-amino-1,2,4-triazole in rats has been shown to decrease voluntary ethanol consumption (Putnam et al., 2000).

In silico studies offer advantages such as rapid execution, low cost, and reduced reliance on animal testing for toxicity assays. Various computational tools provide insights into bioactive substances, including pharmacokinetic properties, biological receptor predictions, and mechanisms of action (Kadam and Roy, 2007; Kazmi et al., 2019; Vanjari et al., 2012). Key pharmacokinetic factors, such as absorption, distribution, metabolism, excretion, and toxicity, are critical in developing substances that can function as bioactives in the body (Cheng et al., 2013).

While the bioactivity of naringenin—both in its free and encapsulated forms—is well characterized in the literature, cytogenetic assessments of cytotoxicity and genotoxicity, along with in silico evaluations, are still in their infancy (Bonciu et al., 2018). Cyto-genotoxicity assays that assess the integrity of the mitotic spindle and chromosomal structure are particularly relevant, as significant changes in cell production may lead to severe disorders, including neoplasms (Sales, 2017).

To our knowledge, there are currently no reports in the scientific literature regarding the cytotoxic, genotoxic, and antigenotoxic potential of naringenin nanoparticles in tissues characterized by intense cell proliferation. Studies investigating the toxicity of naringenin in amphibians have indicated toxic effects at high doses (10 mg/L). Regarding its antiestrogenic properties, naringenin acts through mechanisms mediated by estrogen receptors, exhibiting toxicity at concentrations exceeding 40 mg per individual in rat studies, with no adverse effects reported at lower concentrations (Amin et al., 2020). In contrast, tests in mice demonstrated promising results with a concentration of 200 nmol/kg for the inhibition of lung metastases (Galati and O'Brien, 2004). Additionally, due to the inhibitory effects of naringenin on liver enzymes, the consumption of grapefruit juice may interfere with the metabolism of drugs processed in the liver, potentially altering pharmacokinetics and leading to toxicity (Moghaddam et al., 2020; Karim et al., 2018; Ribeiro, 2011).

The objective of this study was to assess the potential cytotoxic and genotoxic effects of naringenin in both its encapsulated and non-encapsulated forms. First, the pharmacokinetic properties of naringenin were evaluated using Lipinski's Rule of Five, and the AdmetSAR 2.0 tool was employed to predict these properties. Subsequently, molecular docking studies were conducted to elucidate how naringenin interacts with the enzymes superoxide dismutase (SOD2) and catalase.

2. Material and Methods

2.1. Material

Naringenin (98% purity) and Poloxamer 407 were obtained from Sigma-Aldrich and used as received. Tween 80 (analytical standard, Dynamical) was also used to obtain the nanoparticles. Orcein acetic (2%, Dinâmica) served as the dye, and methyl methanesulfonate (MMS) was used as the positive control. Analytical-grade acetone, ethanol, and hydrochloric acid (Synth) were also utilized. Onion bulbs of the *Allium cepa* L. species (beta crystal variety, pear-shaped) were acquired from a local organic garden.

2.2. Production of naringenin nanoparticles

The nanoparticles were obtained using the solid dispersion technique previously described by Almeida et al. (Almeida et al., 2018). Tween 80 (9 mg, stabilizer) and Poloxamer 407 (900 mg, encapsulant) were added to 37.5 g of ethanol, and the mixture was stirred for 10 minutes at 60°C. After cooling to 25°C, naringenin (90 mg) was incorporated, and stirring was maintained for an additional 5 minutes. Sonication was performed using a Fisher Scientific device (120W, 1/8" tip, 120 Hz) for 3 minutes (30 seconds on, 10 seconds off) in an ice bath. The ethanol was then evaporated in a forced-air oven at 40°C for 24 hours. The dried samples were stored at 10°C, protected from light, until further use.

2.3. in silico studies

The ACD/ChemSketch tool was used for structural drawing, SMILES code generation (O=C2c3c(O[C@H](c1ccc(O)cc1)C2)cc(O)cc3O), and three-dimensional determination of naringenin. The molecular structure with optimized three-dimensional arrangement was saved in an individual file with a .mol extension. The ACD/ChemSketch tool, accessible offline, is maintained by ACD/Labs. Molinspiration (free resource available at https://www.molinspiration.com/) was employed for the assessed molecular properties related to oral bioavailability based on Lipinski's rule of five, where the following criteria must be met: miLogP (octanol-water partition coefficient) ≤ 5.00; TPSA (topological polar surface area) ≤ 140 Å^2; MM (molar mass) ≤ 500 g.mol^{-1}; nALH (number of hydrogen bond acceptors) ≤ 10; and nDLH (number of hydrogen bond donors) ≤ 5.

AdmetSAR 2.0 (free tool at http://lmmd.ecust.edu.cn/admetsar2/) was employed to predict pharmacokinetic properties, including absorption, distribution, metabolism, toxicity, and excretion (ADMET). Among the 47 available models, this study considered models for absorption in the human intestine, Caco-2, Ames mutagenesis, hepatotoxicity, and acute oral toxicity. The tool classifies toxicity as positive (+), negative (-), and at different levels (I, II, and III), with higher levels indicating greater activity. The MetaTox tool (free tool at *http://www.way2drug.com/mg*) was utilized for predicting xenobiotic metabolism and calculating the toxicity of metabolites based on the chemical structure of known compounds. MetaTox predicts metabolites formed through nine classes of reactions (aliphatic and aromatic hydroxylation, N- and O-glucuronidation, N-, S-, and C-oxidation, and N- and O-dealkylation). The probability calculation for generated metabolites is based on analyses of structure-biotransformation and modified atomic structure relationships using a Bayesian approach (Rudik et al., 2017). IGEMDOCK 2.1 was used in the molecular docking studies, executed within its Protein Ligand Docking/Screening section. This involved preparing the active site through the Prepare Binding Site function and loading the molecular structure of naringenin stored in the ChemSketch tool. Interaction energies of naringenin with amino acid residues of the studied enzyme were generated on the Docked poses/Post-Screening Analysis page within the program itself (Hsu et al., 2011).

The PDB 1LUV (enzyme superoxide dismutase, SOD2) from the Protein Data Bank was used to evaluate the action of naringenin (Hearn et al., 2003). This enzyme was selected due to its significance in the endogenous antioxidant system and its involvement in mutagenic changes and cytotoxicity induced by external agents. It consists of two chains (A and B) and has a total length of 198 amino acids, derived from *Homo sapiens*. The active site of this enzyme is surrounded by the amino acid residues His26, His30, His74, His163, and Asp159. The catalase enzyme utilized in this study corresponds to Protein Data Bank entry PDB 1DGF Putnam et al. (2000) consists of four chains (A, B, C, and D), with a length of 497 amino acid residues and of *Homo sapiens* origin. The UCSF Chimera tool was used to study the interactions of naringenin and the enzymes.

PoseView, integrated into the Proteins Plus server (free tool at https://proteinsplus.zbh.uni-hamburg.de/#dogsite), automatically generated two-dimensional diagrams of protein-ligand complexes according to chemical drawing conventions based on the 2Ddraw library. Molecular interactions were estimated by an embedded interaction model based on atom types and simple geometric criteria (Fricker et al., 2004).

2.4. Cytotoxicity and genotoxicity analyzes

The *A. cepa* test system is frequently used in cytotoxicity and genotoxicity assessments of natural products of different origins (Herrero et al., 2012; Barros et al., 2023). This test system has high sensitivity, even when compound concentrations are in the nanogram range, and the results obtained have a significant correlation with those obtained in animals, other plants, and *in vitro* (Santo et al., 2023).

For the positive control, 5,000 cells were evaluated. Cells in interphase, prophase, metaphase, anaphase, and telophase were counted to determine the mitotic index,

thus establishing the cytotoxic potential. The cytotoxicity and genotoxicity of naringenin were assessed following the procedures described in the literature with minor modifications (Santo et al., 2023). The concentrations of naringenin used in the aqueous solution were 1% and 3% (w/v), chosen based on previous experiments. Onion bulbs were placed in flasks with distilled water to encourage root growth to approximately 3.0 cm in length. Prior to exposing the roots to their respective concentrations or the negative control (distilled water), the roots were collected and fixed to serve as a baseline control, identified as the 0-hour analysis time (Control - 0h). The remaining roots were then placed in their respective concentrations or controls for exposure periods of 24 and 48 hours. Five onion bulbs were used for each evaluated concentration or control. A positive control was prepared using methyl methanesulfonate (MMS, 4.10^{-4} mol/L), a substance known to be cytotoxic and genotoxic to *Allium cepa*. The five bulbs used for the positive control were exposed to the MMS concentration for only 24 hours. No roots were collected at the 0-hour and 48-hour time points.

The roots collected during the experiment were fixed in a 3:1 Carnoy solution (ethanol: acetic acid) for up to 24 hours. After fixation, the roots were hydrolyzed in 1N HCl, and the meristematic regions were excised to prepare slides using the squash technique. The slides were stained with 2% orcein in acetic acid, following the protocol established by Guerra and Souza (2002). The samples were analyzed using an optical microscope (Zeiss Primo Star with Axiocam 105 Color camera) at 400x magnification. For each bulb, 1,000 cells were analyzed, totaling 5,000 cells for each control of the bulb itself (time 0 hours), each 24-hour exposure group, and each 48-hour exposure group, summing up to 15,000 cells analyzed for each concentration and negative control.

Mitotic index (MI) or cell proliferation index was calculated according to Equation 1, where $cell_{division}$ is the total number of cellular divisions detected and $cell_{total}$ is the total number of cells evaluated in each condition.

$$MI(\%) = 100.\frac{cell_{division}}{cell_{total}} \quad (1)$$

The genotoxic potential was evaluated by assessing the frequency of micronuclei, colchicine metaphases, anaphase and telophase bridges, gene amplifications, cells with adhesions, nuclear buds, and multipolar anaphases. The Index of Cellular Alterations (ICA, Equation 2) for each exposure time was calculated by counting the number of aberrant cells among 100 analyzed cells, resulting in a total of 500 cells analyzed for each time point (0, 24, and 48 hours), yielding a cumulative total of 1500 cells assessed for each concentration and the negative control. For the positive control, 500 cells were also analyzed. In this equation, "cellular changes" refers to the total number of aberrant cell divisions detected, while "total cells" represents the total number of cells evaluated under each condition.

$$ICA(\%) = 100.\frac{cell_{cellular\ changes}}{cell_{total}} \quad (2)$$

2.5. Statistical analysis

Analysis of variance (ANOVA) was conducted to interpret the results obtained from the *in vivo* assays. Mean values were compared using the Scott-Knott test, with a significance level set at 0.05.

3. Results and Discussion

3.1. in silico studies

3.1.1. Evaluation of pharmacokinetic properties of naringenin

The oral bioavailability profile was evaluated using Lipinski's Rule of Five, which considers five key parameters: (1) the number of hydrogen bond acceptor groups (nALH) should be 10 or fewer; (2) the number of hydrogen bond donor groups (nDLH) should be 5 or fewer; (3) the molecular weight should not exceed 500 g/mol; and (4) the LogP (octanol-water partition coefficient) should be 5 or lower. Molecules that violate more than one of these criteria typically encounter challenges related to bioavailability (Veras et al., 2023). Naringenin exhibited the following molecular properties related to oral bioavailability: miLogP = 2.12, TPSA = 86.99 $Å^2$, molecular mass (MM) = 230.26 $g.mol^{-1}$, number of hydrogen bond acceptors (nALH) = 5, and number of hydrogen bond donors (nDLH) = 3. Since none of these parameters violate Lipinski's Rule of Five, naringenin is predicted to have good oral bioavailability.

It's important to note that oral bioavailability is significantly influenced by the metabolism of the bioactive compound, which can result in a considerable reduction in plasma concentration following absorption Felgines et al. (2000) demonstrated that when administered orally to rats, naringenin is extensively esterified to sulfate groups, accounting for approximately 90% of its metabolites. Additionally, naringenin was metabolized into phenolic acids found in plasma and urine, primarily as glucurono- or sulfo-conjugates. Bugianesi et al. (2002) investigated whether plasma levels of naringenin could be detected after consuming a meal containing 150 mg of cooked tomato extract, which equates to 3.8 mg of naringenin. They found that unconjugated naringenin was undetectable in plasma at any time following the meal. In a literature review on the therapeutic potential of naringenin, Salehi et al. (Salehi et al., 2019) highlighted that the compound's bioavailability has been extensively studied, indicating significant pre-systemic metabolism by intestinal flora, which results in a diverse array of degradation products.

This finding suggests that the bioactivities attributed to naringenin in the literature may be due to its metabolites. Understanding the therapeutic effects of naringenin requires consideration of the metabolites produced by intestinal flora and those formed after absorption. The molecular structures of potential naringenin metabolites, calculated using the MetaTox tool, are detailed in Table S1 (Supplementary Material). A total of 20 metabolites were predicted, ranked by their likelihood of formation within the organism. The metabolites with the highest probability of occurrence primarily arise from

glucuronidation (metabolites 1, 2, and 3), sulfonation (metabolites 4, 5, and 6), and hydroxylation (metabolites 7-11). Importantly, the metabolites generated during biotransformation can differ significantly from the parent compound in their bioactivity profiles, potentially resulting in enhanced efficacy, loss of activity, drug-drug interactions, or adverse and toxic effects (Rudik et al., 2017; Rudik et al., 2023).

The parameters related to ADMET processes were studied using the admetSAR tool and are presented in Table 1.

In the Human Intestinal Absorption (HIA) model, naringenin exhibited a positive result, indicating good potential for absorption. Shen et al. (2010) developed this algorithm using data from 578 compounds, of which 500 were classified as absorbed (HIA+) and 78 as not absorbed (HIA-). A compound is labeled HIA- if its calculated HIA% is less than 30%; otherwise, it is categorized as HIA+. Similarly, naringenin showed a positive result in the Caco-2 cell permeability model, which uses Caco-2 cells as an in vitro representation of the human small intestine mucosa to assess the permeability of orally administered drugs. The algorithm for this model, developed by The et al. (2011) analyzed permeability data for 674 substances, including drug-like compounds and commercial drugs. The positive outcomes in both the Caco-2 permeability and HIA models align with the predicted oral bioavailability, serving as crucial indicators for the absorption of bioactive substances.

In terms of hepatotoxicity, naringenin received a positive result at level II. Mulliner et al. (2016) developed the hepatotoxicity algorithm based on a study of 3,115 toxic and 593 non-toxic substances, using data from various publications and databases, including Drugbank (2016). Regarding mutagenicity, a key toxicity model, naringenin, showed a negative result, indicating it is likely non-mutagenic. This model's algorithm was derived from a comprehensive database of 7,617 compounds, including 4,252 mutagenic and 3,365 non-mutagenic substances (Xu et al., 2012). For acute oral toxicity, naringenin demonstrated moderate toxicity, falling into category II (with an LD50 range of 50 $mg.kg^{-1}$ to 500 $mg.kg^{-1}$). This finding and indications of hepatotoxicity highlight the need to establish both the minimum effective dose of naringenin for achieving desired bioactivities and the maximum safe dose to mitigate potential adverse effects. The results from the ADMET property studies suggest that naringenin has relatively low toxicity, making it a promising candidate for developing nutraceuticals and for enhanced applications in the food industry.

Table 1. ADMET properties of the naringenin performed in admetSAR.

Models evaluated	Value	Probability
Absorption in the human intestine	+	0.9936
Caco-2	+	0.5424
Mutagenesis according to Ames	-	0.8700
Hepatotoxicity	+	0.6750
Acute Oral Toxicity	II	0.3682

3.1.2. Enzyme superoxide dismutase (SOD2, PDB 1LUV)

Figure 1a displays chain A of the SOD2 enzyme, emphasizing the active site region surrounding two Mn^{2+} ions. Figure 1b illustrates the optimal pose, representing naringenin's lowest energy molecular docking result against SOD2 (PDB 1LUV). In Figure 1c, it is evident that naringenin is positioned within a hydrophilic region, forming hydrogen bonds with the amino acid residues Asp105, Thr112, and Asn182, while also engaging in van der Waals interactions with Lys178 and Trp181 (Hearn et al., 2003).

The interaction between naringenin and SOD2 (PDB 1LUV) yielded a free energy of -81.42 $kJ.mol^{-1}$, with -59.66 $kJ.mol^{-1}$ attributed to van der Waals interactions and - 21.76 $kJ.mol^{-1}$ resulting from hydrogen bonding interactions.

Figure 1. Molecular Docking results of the enzyme superoxide dismutase (SOD2, PDB 1LUV). (a) Representation of the A chain of the SOD2 enzyme (PDB 1LUV) with emphasis (red circles) on the active site regions; (b) Best pose resulting from the molecular anchoring study of naringenin against SOD2 (PDB 1LUV); (c) Two-dimensional representation, produced by the Pose View tool, of the interaction between the SOD2 enzyme (PDB 1LUV) and naringenin.

In examining the hydrophobic surface of the complex formed between the enzyme SOD2 and naringenin (Figure 1b), naringenin is anchored to the enzyme's surface. The red regions indicate hydrophobic areas, while the blue regions denote hydrophilicity. Naringenin is located within a hydrophilic region, forming hydrogen bonds with the amino acid residues Asp105, Thr112, and Asn182, and engages in van der Waals interactions with Lys178 and Trp181. Additionally, the amino acid residue His30, located in the substrate access channel and approximately 5.8 Å from Mn (III), plays a crucial role in enzymatic activity. Other important residues in the active site, such as His26, His74, His163, and Asp159, are also essential for the catalytic function of SOD2 (Hearn et al., 2003). Notably, naringenin is anchored in a region that is distant from the enzyme's active site, where manganese is present and plays a crucial role. This spatial arrangement suggests a non-competitive interaction mechanism, indicating that naringenin may affect the enzyme's activity without directly competing with the substrate for the active site (Cheng and Prusoff, 1973).

3.1.3. Enzyme catalase (PDB 1DGF)

Figure 2 presents the interactions between the heme iron and the amino acid residues located in the catalase's active site (left side). On the right side, the figure details the interactions between naringenin and the amino acid residues in the anchoring region.

The interaction between naringenin and catalase (PDB 1DGF) resulted in a free energy of 114.59 kJ.mol^{-1}, comprising -95.37 kJ.mol^{-1} from van der Waals interactions and -19.22 kJ.mol^{-1} from hydrogen bonding. Naringenin interacts with several amino acid residues that are crucial for catalase's catalytic process, including Arg72, Arg112, Thr361, and Tyr385. This suggests that naringenin may act as a competitive inhibitor of catalase.

3.2. in vivo studies

Tables 2 and 3 present the results obtained in assays with A. cepa exposed to free (non-encapsulated) naringenin and naringenin nanoparticles. Based on these tables, can be seen that naringenin in the three concentrations evaluated, free and encapsulated, did not cause changes in the cell division of the meristematic cells of A. cepa roots, demonstrating mitotic indices and cellular alterations equal to the negative control, in the 24 and 48 hours of exposure. Therefore, in the concentrations and conditions evaluated, naringenin was neither cytotoxic nor genotoxic. It iso worth pointing out that the Mitotic Index (MI) and the Index of cellular alterations (ICA) of methyl methanesulfonate (MMS, positive control) at 4x10^{-4} mol.L^{-1} and after 24 h exposure time was 6.51 ± 0.34% and 8.95 ± 0.98%, respectively.

The results demonstrating the non-cytotoxicity and genotoxicity of naringenin encapsulated at concentrations of 1% and 3% are quite promising, as the nanoparticles did not disrupt cell division dynamics, and cell homeostasis was maintained. The antioxidant enzymes catalase (CAT) and superoxide dismutase (SOD) play crucial roles in cellular proliferation. Their activity in tissues with high rates of cell division, where cellular metabolism largely focuses on producing new cells, helps maintain homeostasis by regulating the production of superoxide and hydroxyl radicals (Santo et al., 2023). Excess radicals in cells can denature proteins and enzymes, including those in cell membranes and those associated with assembling the mitotic spindle. This disruption can impair the precise movement of chromosomes during mitosis, as well as affect DNA duplication, cytoplasmic division, and the proper condensation of chromatin (Dias and Vale Júnior, 2019). Such events are crucial for producing identical cells during each cell cycle, which is essential for the growth and development of various organs (Ferreira et al., 2022).

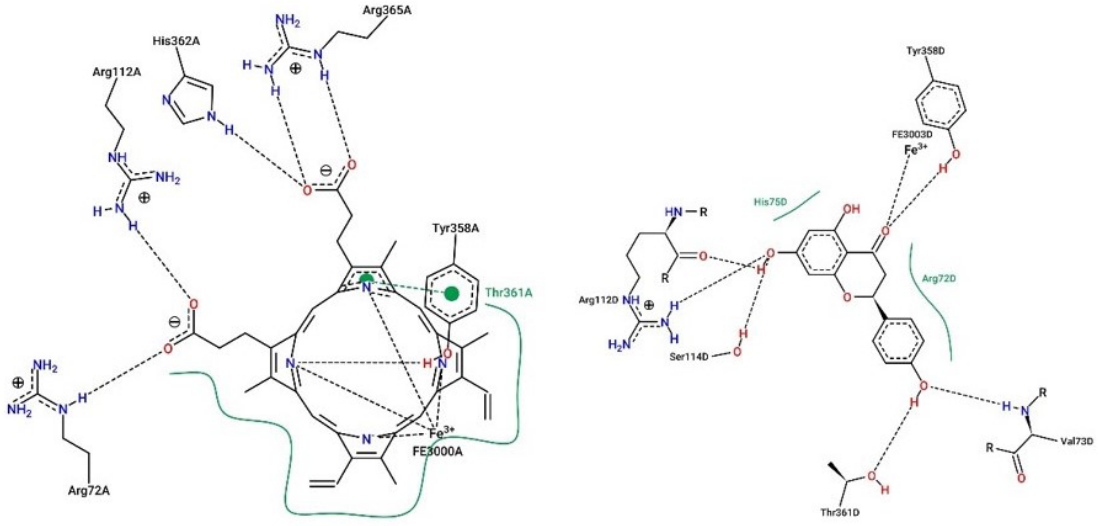

Figure 2. Two-dimensional representation of the interaction between catalase (PDB 1DGF) and naringenin.

Table 2. Mitotic index (MI, %) observed in *A. cepa* root meristems exposed to different concentrations of free naringenin at different exposure times.

Naringenin Concentration (wt%)	Mitotic Index (MI, %)		
	0 h (Control)	24 h	48 h
1	22.0 ± 0.7 [a]	27.1 ± 1.0 [a]	28.4 ± 0.8 [a]
3	24.0 ± 0.2 [a]	21.2 ± 0.7 [a]	21.7 ± 0.6 [a]
Naringenin nanoparticles concentration (wt%)			
1	19.8 ± 0.50 [a]	18.7 ± 0.70 [a]	20.9 ± 0.30 [a]
3	18.0 ± 0.98 [a]	16.9 ± 0.89 [a]	20.9 ± 0.35 [a]

Analysis of variance (ANOVA). Observed means compared by Scott-Knott test at 0.05. Different lowercase letters refer to different means between the considered exposure times at the same concentration. The statistics of the naringenin and naringenin nanoparticles were evaluated separately.

Table 3. Index of cellular alterations (ICA) observed in root meristems of *A. cepa* exposed to different concentrations of free naringenin at different exposure times.

Naringenin Concentration (wt%)	Index of cellular alterations (ICA, %)		
	0 h (Control)	24 h	48 h
1	0.10 ± 0.09[a]	010 ± 0.08 [a]	0.10 ± 0.08 [a]
3	0.10 ± 0.08[a]	0.10 ± 0.07 [a]	0.10 ± 0.09 [a]
Naringenin nanoparticles concentration (wt%)			
1	0.20 ± 0.1[a]	0.20 ± 0.1[a]	0.60 ± 0.2[a]
3	0.20 ± 0.1[a]	0.20 ± 0.1[a]	0.60 ± 0.2[a]

Analysis of variance (ANOVA). Observed means compared by Scott-Knott test at 0.05. Different letters in the same line indicate significantly different mean values between the considered exposure times at the same concentration. The statistics of the naringenin and naringenin nanoparticles were evaluated separately.

Based on the *in silico* studies, free naringenin was identified as a competitive inhibitor of catalase (CAT) while demonstrating a high potential to bind to superoxide dismutase (SOD). The activation of SOD helps to explain the absence of cytotoxicity and genotoxicity of naringenin toward the root meristems of *Allium cepa* (Table 2 and 3), as SOD activation regulates the production of hydrogen peroxide and superoxide species in cells.

This suggests that naringenin may enhance the cell defense system, promoting a protective effect on tissue. Ganaie et al. (2019) conducted a study to investigate the protective effects of naringenin against DNA damage induced by oxaliplatin in mice. Their results showed that administering naringenin significantly reduced the DNA damage caused by oxaliplatin, likely attributable to its potent antioxidant properties.

4. Conclusions

Naringenin was evaluated for potential cytotoxicity, genotoxicity, and mutagenicity using the meristematic tissues of *Allium cepa* L., alongside in silico studies to determine pharmacokinetic parameters and assess molecular docking interactions with the enzyme's superoxide dismutase 2 (SOD2, PDB 1LUV) and catalase (PDB 1DGF). The results indicated that naringenin, both in its free and nanoparticle forms, did not alter the cell division index of meristematic cells in *A. cepa* roots under the tested conditions. Furthermore, no significant changes in mitotic spindle structure or chromosomal breaks were observed.

The molecular docking study of naringenin and SOD2 showed that naringenin is anchored in a hydrophilic region, away from the enzyme's active site, forming hydrogen bonds and van der Waals interactions with specific amino acid residues. This suggests a non-competitive inhibition mechanism, with a calculated free energy of -81.42 kJ.mol^{-1}, comprising -59.66 kJ.mol^{-1} from van der Waals interactions and -21.76 kJ.mol^{-1} from hydrogen bonds. The ADMET properties studies indicated that naringenin has relatively low toxicity, aligning with the in vivo findings.

Conversely, the docking study of naringenin with catalase yielded a free energy of -114.587 kJ.mol^{-1}, resulting from -95.371 kJ.mol^{-1} of van der Waals interactions and -19.2166 kJ.mol^{-1} from hydrogen bonding. Naringenin interacted with several amino acid residues crucial for catalase's catalytic activity, such as Arg72, Arg112, Thr361, and Tyr385, suggesting it may act as a competitive catalase inhibitor.

Overall, the in vivo assays on meristematic tissues of *Allium cepa* L., combined with the ADMET properties results, indicate that naringenin possesses molecular characteristics favorable for orally administered bioactive substances and exhibits relatively low toxicity. These attributes position naringenin as a promising candidate for developing new nutraceuticals and greater integration into the food industry.

Acknowledgements

Authors would like to thank CAPES for the financial support (Project 0001), CNPq for the scholarships, and also CAMulti-CM laboratory for the analyses.

References

ALMEIDA, H.H.S., BARROS, L., BARREIRA, J.C.M., CALHELHA, R.C., HELENO, S.A., SAYER, C., MIRANDA, C.G., LEIMANN, F.V., BARREIRO, M.F. and FERREIRA, I.C.F.R., 2018. Bioactive evaluation and application of different formulations of the natural colorant curcumin (E100) in a hydrophilic matrix (yogurt). *Food Chemistry*, vol. 261, pp. 224-232. http://doi.org/10.1016/j.foodchem.2018.04.056. PMid:29739587.

AMIN, I., MAJID, S., FAROOQ, A., WANI, H.A., NOOR, F., KHAN, R., SHAKEEL, S., BHAT, S.A., AHMAD, A., MADKHALI, H., AHMAD, M. and REHMAN, M.U., 2020. Naringenin (4,5,7-trihydroxyflavanone) as a potent neuroprotective agent: from chemistry to medicine. *Studies in Natural Products Chemistry*, vol. 65, pp. 271-300. http://doi.org/10.1016/B978-0-12-817905-5.00008-1.

BARROS, D.G.C., NASCIMENTO, G.C.S.G., OKON, C., ROCHA, M.B., SANTO, D.E., FEITOZA, L.L., VALARINI JUNIOR, O., GONZALEZ, R.S., SOUZA, D.C. and PERON, A.P., 2023. Benzophenone-3 sunscreen causes phytotoxicity and cytogenotoxicity in higher plants. *Environmental Science and Pollution Research International*, vol. 30, no. 52, pp. 112788-112798. http://doi.org/10.1007/s11356-023-30365-3.

BONCIU, E., FIRBAS, P., FONTANETTI, C.S., WUSHENG, J., KARAISMAILOĞLU, M.C., LIU, D., MENICUCCI, F., PESNYA, D.S., POPESCU, A., ROMANOVSKY, A.V., SCHIFF, S., ŚLUSARCZYK, J., DE SOUZA, C.P., SRIVASTAVA, A., SUTAN, A. and PAPINI, A., 2018. An evaluation for the standardization of the Allium cepa test as cytotoxicity and genotoxicity assay. *Caryologia*, vol. 71, no. 3, pp. 191-209. http://doi.org/10.1080/00087114.2018.1503496.

BUGIANESI, R., CATASTA, G., SPIGNO, P., D'UVA, A. and MAIANI, G., 2002. Naringenin from cooked tomato paste is bioavailable in men. *The Journal of Nutrition*, vol. 132, no. 11, pp. 3349-3352. http://doi.org/10.1093/jn/132.11.3349. PMid:12421849.

CAVIA-SAIZ, M., BUSTO, M.D., PILAR-IZQUIERDO, M.C., ORTEGA, N., PEREZ-MATEOS, M. and MUÑIZ, P., 2010. Antioxidant properties, radical scavenging activity and biomolecule protection capacity of flavonoid naringenin and its glycoside naringin: A comparative study. *Journal of the Science of Food and Agriculture*, vol. 90, no. 7, pp. 1238-1244. http://doi.org/10.1002/jsfa.3959. PMid:20394007.

CHAURASIA, S., PATEL, R.R., VURE, P. and MISHRA, B., 2018. Potential of cationic-polymeric nanoparticles for oral delivery of naringenin: in vitro and in vivo investigations. *Journal of Pharmaceutical Sciences*, vol. 107, no. 2, pp. 706-716. http://doi.org/10.1016/j.xphs.2017.10.006. PMid:29031951.

CHENG, F., LI, W., LIU, G. and TANG, Y., 2013. In silico ADMET prediction: recent advances, current challenges and future trends. *Current Topics in Medicinal Chemistry*, vol. 13, no. 11, pp. 1273-1289. http://doi.org/10.2174/15680266113139990033. PMid:23675935.

CHENG, Y.-C. and PRUSOFF, W.H., 1973. Relationship between the inhibition constant (K1) and the concentration of inhibitor which causes 50 per cent inhibition (I50) of an enzymatic reaction. *Biochemical Pharmacology*, vol. 22, no. 23, pp. 3099-3108. http://doi.org/10.1016/0006-2952(73)90196-2. PMid:4202581.

DIAS, W.L.F. and VALE JUNIOR, E.P., 2019. Cytogenotoxic effect, phytochemical screening and antioxidant potential of Jatropha mollissima (Pohl) Baill leaves. *South African Journal of Botany*, vol. 123, pp. 30-35. http://doi.org/10.1016/j.sajb.2019.02.007.

DRUGBANK, 2016 [viewed 18 July 2006]. *Drugbank* [online]. Available from: https://www.drugbank.com

FELGINES, C., TEXIER, O., MORAND, C., MANACH, C., SCALBERT, A., RÉGERAT, F. and RÉMÉSY, C., 2000. Bioavailability of the flavanone naringenin and its glycosides in rats. *American Journal of Physiology. Gastrointestinal and Liver Physiology*, vol. 279, no. 6, pp. 1148-1154. http://doi.org/10.1152/ajpgi.2000.279.6.G1148. PMid:11093936.

FERREIRA, P.M.P., SOUSA, I.J.O., MACHADO, K.N., DA SILVA NETO, L.A., DE FREITAS, M.M., DOS SANTOS, I.L., DO NASCIMENTO RODRIGUES, D.C., DE SOUSA, R.W.R., DOS REIS, A.C., DO NASCIMENTO, M.L.L.B., DE MENEZES, A.-A.P.M., DO NASCIMENTO, A.M., DE OLIVEIRA FERREIRA, J.R., PERON, A.P. and DE CASTRO E SOUSA, J.M., 2022. Antimitotic and toxicogenetic action of *Stevia urticifolia* aerial parts on proliferating vegetal and mammalian cells: *in vitro* and *in vivo* traditional and replacement methods. *Journal of Toxicology and Environmental Health. Part A.*, vol. 85, no. 18, pp. 750-766. http://doi.org/10.1080/15287394.2022.2081640. PMid:35698798.

FLYNN, J.M. and MELOV, S., 2013. SOD2 in mitochondrial dysfunction and neurodegeneration. *Free Radical Biology & Medicine*, vol. 62, pp. 4-12. http://doi.org/10.1016/j.freeradbiomed.2013.05.027. PMid:23727323.

FRICKER, P.C., GASTREICH, M. and RAREY, M., 2004. Automated drawing of structural molecular formulas under constraints. *Journal of Chemical Information and Computer Sciences*, vol. 44, no. 3, pp. 1065-1078. http://doi.org/10.1021/ci049958u. PMid:15154775.

GALATI, G. and O'BRIEN, P.J., 2004. Potential toxicity of flavonoids and other dietary phenolics: significance for their chemopreventive and anticancer properties. *Free Radical Biology & Medicine*, vol. 37, no. 3, pp. 287-303. http://doi.org/10.1016/j.freeradbiomed.2004.04.034. PMid:15223063.

GANAIE, M.A., JAN, B.L., KHAN, T.H., ALHARTHY, K.M. and SHEIKH, I.A., 2019. The protective effect of naringenin on oxaliplatin-induced genotoxicity in mice. *Chemical & Pharmaceutical Bulletin*, vol. 67, no. 5, pp. 433-438. http://doi.org/10.1248/cpb.c18-00809. PMid:30787216.

GUERRA, M. and SOUZA, M.J., 2002. *Como observar cromossomos: um guia de técnicas em citogenética vegetal, animal e humana.* Ribeirão Preto: FUNPEC.

HEARN, A.S., STROUPE, M.E., CABELLI, D.E., RAMILO, C.A., LUBA, J.P., TAINER, J.A., NICK, H.S. and SILVERMAN, D.N., 2003. Catalytic and structural effects of amino acid substitution at histidine 30 in human manganese superoxide dismutase: insertion of valine Cγ into the substrate access channel. *Biochemistry*, vol. 42, no. 10, pp. 2781-2789. http://doi.org/10.1021/bi0266481. PMid:12627943.

HERRERO, O., PÉREZ MARTÍN, J., FERNÁNDEZ FREIRE,, P., CARVAJAL LÓPEZ, L., PEROPADRE, A. and HAZEN, M.J., 2012. Toxicological evaluation of three contaminants of emerging concern by use of the *Allium cepa* test. *Mutation Research/Genetic Toxicology and Environmental Mutagenesis*, vol. 743, no. 1-2, pp. 20-24. http://doi.org/10.1016/j.mrgentox.2011.12.028.

HSU, K.C., CHEN, Y.F., LIN, S.R. and YANG, J.M., 2011. Igemdock: A graphical environment of enhancing gemdock using pharmacological interactions and post-screening analysis. *BMC Bioinformatics*, vol. 12, no. Suppl 1, suppl. 1, pp. S33. http://doi.org/10.1186/1471-2105-12-S1-S33. PMid:21342564.

JOHNSON, F. and GIULIVI, C., 2005. Superoxide dismutases and their impact upon human health. *Molecular Aspects of Medicine*, vol. 26, no. 4-5, pp. 340-352. http://doi.org/10.1016/j.mam.2005.07.006. PMid:16099495.

KADAM, R. and ROY, N., 2007. Recent trends in drug-likeness prediction: a comprehensive review of in silico methods. *Indian Journal of Pharmaceutical Sciences*, vol. 69, no. 5, pp. 609-615. http://doi.org/10.4103/0250-474X.38464.

KARIM, N., JIA, Z., ZHENG, X., CUI, S. and CHEN, W., 2018. A recent review of citrus flavanone naringenin on metabolic diseases and its potential sources for high yield-production. *Trends in Food Science & Technology*, vol. 79, pp. 35-54. http://doi.org/10.1016/j.tifs.2018.06.012.

KAZMI, S.R., JUN, R., YU, M.S., JUNG, C. and NA, D., 2019. In silico approaches and tools for the prediction of drug metabolism and fate: A review. *Computers in Biology and Medicine*, vol. 106, pp. 54-64. http://doi.org/10.1016/j.compbiomed.2019.01.008. PMid:30682640.

KERDUDO, A., DINGAS, A., FERNANDEZ, X. and FAURE, C., 2014. Encapsulation of rutin and naringenin in multilamellar vesicles for optimum antioxidant activity. *Food Chemistry*, vol. 159, pp. 12-19. http://doi.org/10.1016/j.foodchem.2014.03.005. PMid:24767021.

LIPINSKI, C.A., 2004. Lead- and drug-like compounds: the rule-of-five revolution. *Drug Discovery Today. Technologies*, vol. 1, no. 4, pp. 337-341. http://doi.org/10.1016/j.ddtec.2004.11.007. PMid:24981612.

MAATOUK, M., ELGUEDER, D., MUSTAPHA, N., CHAABAN, H., BZÉOUICH, I.M., LOANNOU, I., KILANI, S., GHOUL, M., GHEDIRA, K. and CHEKIR-GHEDIRA, L., 2016. Effect of heated naringenin on immunomodulatory properties and cellular antioxidant activity. *Cell Stress & Chaperones*, vol. 21, no. 6, pp. 1101-1109. http://doi.org/10.1007/s12192-016-0734-0. PMid:27623863.

MANCHOPE, M.F., CALIXTO-CAMPOS, C., COELHO-SILVA, L., ZARPELON, A.C., PINHO-RIBEIRO, F.A., GEORGETTI, S.R., BARACAT, M.M., CASAGRANDE, R. and VERRI JUNIOR, W.A., 2016. Naringenin inhibits superoxide anion-induced inflammatory pain: role of oxidative stress, cytokines, Nrf-2 and the no-cGMP-PKG-KATP channel signaling pathway. *PLoS One*, vol. 11, no. 4, e0153015. http://doi.org/10.1371/journal.pone.0153015. PMid:27045367.

MCCLEMENTS, D.J., 2018. Recent developments in encapsulation and release of functional food ingredients: delivery by design. *Current Opinion in Food Science*, vol. 23, pp. 80-84. http://doi.org/10.1016/j.cofs.2018.06.008.

MOGHADDAM, R.H., SAMIMI, Z., MORADI, S.Z., LITTLE, P.J., XU, S. and FARZAEI, M.H., 2020. Naringenin and naringin in cardiovascular disease prevention: a preclinical review. *European Journal of Pharmacology*, vol. 887, pp. 173535. http://doi.org/10.1016/j.ejphar.2020.173535. PMid:32910944.

MULLINER, D., SCHMIDT, F., STOLTE, M., SPIRKL, H.P., CZICH, A. and AMBERG, A., 2016. Computational models for human and animal hepatotoxicity with a global application scope. *Chemical Research in Toxicology*, vol. 29, no. 5, pp. 757-767. http://doi.org/10.1021/acs.chemrestox.5b00465. PMid:26914516.

PUTNAM, C.D., ARVAI, A.S., BOURNE, Y. and TAINER, J.A., 2000. Active and inhibited human catalase structures: ligand and NADPH binding and catalytic mechanism. *Journal of Molecular Biology*, vol. 296, no. 1, pp. 295-309. http://doi.org/10.1006/jmbi.1999.3458. PMid:10656833.

RIBEIRO, M.H., 2011. Naringinases: Occurrence, characteristics, and applications. *Applied Microbiology and Biotechnology*, vol. 90, no. 6, pp. 1883-1895. http://doi.org/10.1007/s00253-011-3176-8. PMid:21544655.

RUDIK, A.V., BEZHENTSEV, V.M., DMITRIEV, A.V., DRUZHILOVSKIY, D.S., LAGUNIN, A.A., FILIMONOV, D.A. and POROIKOV, V.V., 2017. Metatox: web application for predicting structure and toxicity of xenobiotics' metabolites. *Journal of Chemical Information and Modeling*, vol. 57, no. 4, pp. 638-642. http://doi.org/10.1021/acs.jcim.6b00662. PMid:28345905.

RUDIK, A.V., DMITRIEV, A.V., LAGUNIN, A.A., FILIMONOV, D.A. and POROIKOV, V.V., 2023. MetaTox 2.0: estimating the biological activity spectra of drug-like compounds taking into account probable biotransformations. *ACS Omega*, vol. 8, no. 48, pp. 45774-45778. http://doi.org/10.1021/acsomega.3c06119. PMid:38075828.

SALEHI, B., FOKOU, P.V.T., SHARIFI-RAD, M., ZUCCA, P., PEZZANI, R., MARTINS, N. and SHARIFI-RAD, J., 2019. The therapeutic potential of naringenin: a review of clinical trials. *Pharmaceuticals (Basel, Switzerland)*, vol. 12, no. 1, pp. 1-18. http://doi.org/10.3390/ph12010011. PMid:30634637.

SALES, I.M.S., 2017. Acute toxicity of grape, plum and orange synthetic food flavourings evaluated in vivo test systems. *Food Technology and Biotechnology*, vol. 55, no. 1, pp. 131-137. http://doi.org/10.17113/ftb.55.01.17.4770. PMid:28559742.

SANTO, D.E., DUSMAN, E., ROMERO, A.L., GONZALES, R.S. and PERON, A.P., 2023. Prospecting toxicity of octocrylene in Allium cepa L. and Eisenia fetida Sav. *Environmental Science and Pollution Research International*, vol. 30, no. 3, pp. 8257-8268. http://doi.org/10.1007/s11356-022-22795-2. PMid:36053420.

SHEN, J., CHENG, F., XU, Y., LI, W. and TANG, Y., 2010. Estimation of ADME properties with substructure pattern recognition. *Journal of Chemical Information and Modeling*, vol. 50, no. 6, pp. 1034-1041. http://doi.org/10.1021/ci100104j. PMid:20578727.

SILVA, S.P., MARQUES, T.S., LANDO, V.R. and ZANI, V.T., 2021. Determinação de polifenóis totais e flavonoides em Eugenia uniflora l. (PITANGA): fruto in natura, polpa congelada e geleia / Determination of total polyphenols and flavonoids in Eugenia uniflora l. (surinam cherry): fresh fruit, frozen pulp and jelly. *Brazilian Journal of Health Review*, vol. 4, no. 6, pp. 28471-28483. http://doi.org/10.34119/bjhrv4n6-393.

SUMATHI, R., TAMIZHARASI, S. and SIVAKUMAR, T., 2015. Bio-dynamic activity of naringenin-a review. *International Journal of Current Advanced Research*, vol. 4, no. 8, pp. 234-236.

THE, H.P., GONZÁLEZ-ÁLVAREZ, I., BERMEJO, M., SANJUAN, V.M., CENTELLES, I., GARRIGUES, T.M. and CABRERA-PÉREZ, M.Á., 2011. In silico prediction of caco-2 cell permeability by a classification QSAR approach. *Molecular Informatics*, vol. 30, no. 4, pp. 376-385. http://doi.org/10.1002/minf.201000118. PMid:27466954.

VANJARI, S., CHIMANDARE, N. and GANDHI, S., 2012. A review on in silico approach in pharmacology. *Adv Res Pharm Biol*, vol. 2, no. 2, pp. 129-141.

VERAS, B.A.F., HUANCA, P.I.J., DE SOUSA OLIVEIRA, I., MAIA, R.T., SILVA SOUZA, H.D. and FERREIRA, S.B., 2023. In silico pharmacological prediction of substituted aminonitriles. *Chemistry Proceedings*, vol. 14, no. 1, pp. 29. http://doi.org/10.3390/ecsoc-27-16178

VEZZA, T., RODRÍGUEZ-NOGALES, A., ALGIERI, F., UTRILLA, M.P., RODRIGUEZ-CABEZAS, M.E. and GALVEZ, J., 2016. Flavonoids in inflammatory bowel disease: a review. *Nutrients*, vol. 8, no. 4, pp. 211. http://doi.org/10.3390/nu8040211. PMid:27070642.

XU, C., CHENG, F., CHEN, L., DU, Z., LI, W., LIU, G., LEE, P.W. and TANG, Y., 2012. In silico prediction of chemical ames mutagenicity. *Journal of Chemical Information and Modeling*, vol. 52, no. 11, pp. 2840-2847. http://doi.org/10.1021/ci300400a. PMid:23030379.

Supplementary Material

Supplementary material accompanies this paper.

Table S1 - Metabolites formed from naringenin as predicted by MetaTox tool.

This material is available as part of the online article from https://doi.org/10.1590/1519-6984.290560